# Characterization of dilute InPN layers grown by liquid phase epitaxy

T. D. Das, S. Dhar, and B. M. Arora

---

---

# Characterization of dilute InPN layers grown by liquid phase epitaxy

T. D. Das,[1] S. Dhar,[1,a)] and B. M. Arora[2]
[1]*Department of Electronic Science, University of Calcutta, 92 A. P. C. Road, Kolkata-700009, India*
[2]*Department of Condensed Matter Physics, Tata Institute of Fundamental Research, Homi Bhabha Road, Mumbai-400005, India*

We have grown dilute InPN layers by liquid phase epitaxy and characterized them using high resolution x-ray diffraction, optical absorption, low temperature photoluminescence, and Hall measurement techniques. Our results indicate that a maximum amount of 0.2% nitrogen has been incorporated in the material with a band gap lowering consistent with expectations. The crystalline quality of the material is found to improve upon nitrogen incorporation. Large increase in luminescence from the material is observed after a high temperature annealing. © *2008 American Institute of Physics*. [DOI: 10.1063/1.3028998]

## I. INTRODUCTION

III–V semiconductors containing small amounts of nitrogen, popularly known as "dilute nitrides," have been of great interest since the beginning of the past decade. The major interest in such materials lies in the fact that the incorporation of a little amount of nitrogen in the host III–V lattice results in a substantial reduction in the band gap of the material, accompanied by an increase in the lattice constant.[1] Change in lattice constant enables the material to be lattice matched to a particular substrate whereas band gap tuning by controlled nitrogen incorporation opens up the potential for application in light emitters in a selected wavelength region and in multilayer solar cells. Dilute GaAsN (Refs. 2–4) and InGaAsN (Refs. 5–7) have been studied most for their promising applications in optoelectronic devices. Band gap reduction effect has also been observed in AlGaAsN,[8] GaPN,[9] GaSbN,[10] InAsN,[11] InAsPN,[12] and InPN.[13] Metal-organic vapor phase epitaxy, gas source molecular beam epitaxy, and, in some limited cases, nitrogen ion implantation have been used for the growth or formation of these materials. InPN has been least studied, presumably because the nitrogen incorporation in InP has been found to be less than 1%,[14,15] a value substantially lower than that obtained in other group III–V-N materials. This low value of nitrogen incorporation is attributed to the very high equilibrium nitrogen vapor pressure over InN and relatively smaller In–N bond strength compared to that of InP.[14] Debbichi *et al.*[16] used a theoretical model to investigate the electronic and vibrational properties of InP and their study predicted that even in the nitrogen content range up to 1%, there will be a substantial reduction in the energy band gap making InPN a potential candidate for realizing long wavelength optoelectronic devices. We have earlier reported a liquid phase epitaxy (LPE) technique for the growth of dilute nitrides and have successfully demonstrated the growth of GaAsN,[17,18] GaSbN,[19] and InAsN.[20] We have used the same technique for the growth of InPN layers and studied their properties. The details of the study are being presented in this paper.

## II. EXPERIMENTAL

We have used a horizontal LPE reactor for the growth of InPN layers on ⟨100⟩ oriented Fe-doped semi-insulating InP substrates. Initially 99.9999% In metal was cleaned and etched following the usual procedures and then loaded in the LPE boat made of high density graphite. The metal was baked at 730 °C for 20 h under a continuous flow of Pd-diffused ultrapure hydrogen gas. Next, required quantities of polycrystalline InN powder of 99.98% purity was added to the baked In and heated again under hydrogen for a period of 1 h at temperatures of 700–720 °C. Finally the In+InN mix was placed over a cleaned and etched polycrystalline InP wafer and baked for 2 h at 650 °C to completely saturate In with phosphorous. After the saturation procedure, the melt was moved away from the InP wafer and baked further at 700 °C for 10 h. Growth was typically done for 5–10 min under a melt supersaturation of 4–5 °C and a constant cooling rate of 0.4–0.5 °C. The same melt was used for 3–4 more growth runs and before each run, additional amount of InN was added to the melt and baked to completely dissolve the same. We have also grown some undoped InP layers for comparison, using the same procedure described above, except the addition of InN. The undoped layer is *n*-type with an electron concentration of $4 \times 10^{16}$ cm$^{-3}$ and mobility around 4500 cm$^2$/V s, as measured by Hall technique to be described later.

The thickness of the grown layers was measured under an Olympus Nomarski Interference Contrast microscope, fitted with a calibrated eye piece. The typical thickness was in the range 4–5 $\mu$m. Characterization was done by high resolution x-ray diffraction (HRXRD), optical absorption, and low temperature photoluminescence (PL) techniques. XRD studies were done in a high resolution x-ray diffractometer under copper $K\alpha$ radiation. Optical absorption studies were done on samples, with the substrate side thinned at room temperatures in a Carry 5000 UV-visible-IR spectrophotometer. PL experiments were done at 18 K. The sample was illuminated by the 488 nm light from an argon ion laser. PL signal from the sample was collected in a McPherson 1-m monochromator and detected in a Si photodetector using the conventional lock-in techniques.
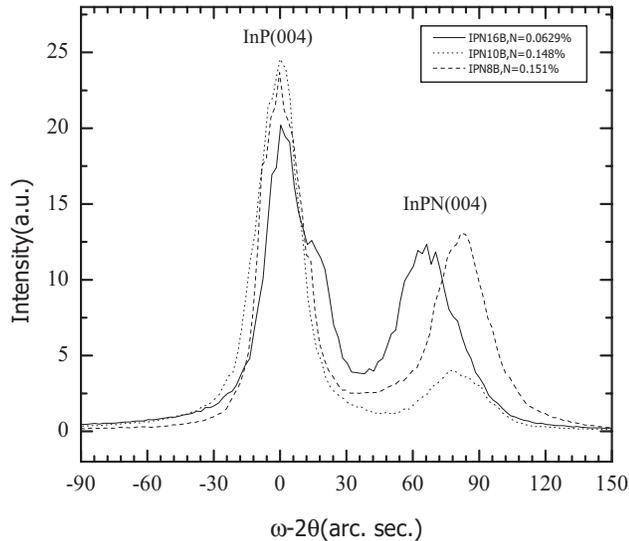
a)Electronic mail: sdhar_25@yahoo.co.in.

FIG. 1. HRXRD curves for three LPE-grown InPN samples containing varying amounts of nitrogen.



FIG. 2. Optical absorption spectra for LPE InPN with different nitrogen contents.

Finally, Hall effect measurements were done on the samples using the van der Pauw technique. For this purpose, layers grown on semi-insulating substrates were cut as 5 × 5 mm$^2$ squares and annealed 90% In + 10% Sn Ohmic contacts were fabricated at the four corners. Measurements were done under a magnetic field of 3 kG.

## III. RESULTS AND DISCUSSIONS

### A. HRXRD

HRXRD curves for three InPN samples are being shown in Fig. 1. Each curve shows two sharp peaks, one due to the layer and other due to the substrate. From the angular separation of the two peaks, we are able to calculate the increase in lattice constant due to nitrogen incorporation. From these data, the nitrogen content in the materials are computed using Vegard's law. The nitrogen content, so computed, are shown in the box of Fig. 1.

### B. Optical absorption

The product of the square of optical absorption coefficient ($\alpha$) and the photon energy are plotted as a function of photon energy for three InPN samples grown from melts with successively increasing amounts of InN. These data are shown in Fig. 2. Energy gap for each sample, obtained from the linear extrapolation of the rising part, is used to calculate the nitrogen content in the material. Nitrogen content of 0.2%, computed from the absorption data, is the maximum value that we have so far been able to introduce in our LPE grown samples.

There have been numerous attempts to explain the band structure properties of the group III–V-N alloys. It is now well established that the properties of the conduction band in these materials can be parametrized in terms of the band anticrossing (BAC) model.[21] According to the BAC model, the interaction of the conduction band edge with the highly
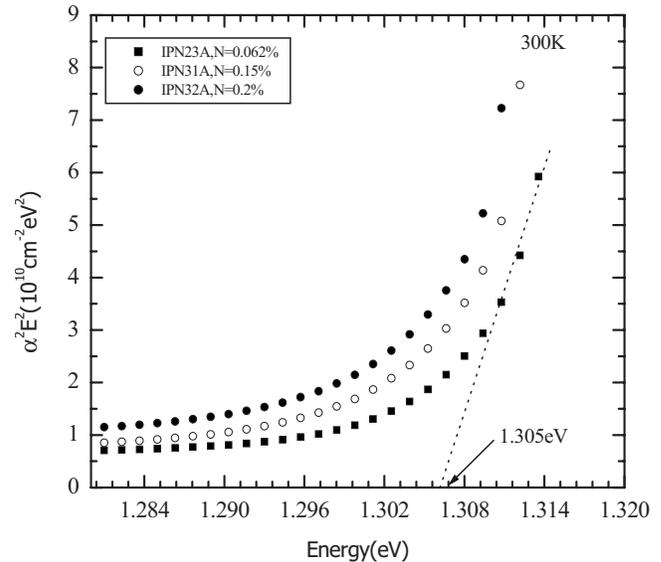
localized N states leads to a splitting of the conduction band into two highly nonparabolic subbands $E_-$ and $E_+$ with dispersion relation given by[22]

$$E_{\pm}(k) = [E_M(k) + E_N] \pm \sqrt{[E_M(k) - E_N]^2 + 4V_{NM}^2}, \qquad (1)$$

where $E_N$ is the position of the nitrogen isoelectronic impurity level in the band structure, $E_M(k)$ is the dispersion relation for the conduction band of the N-free semiconductor matrix, and $V_{NM}$ is the matrix element describing the coupling between the host conduction band ($E_M$) and the resonant nitrogen level ($E_N$) and has the fundamental form $V_{NM} = C_{NM}\sqrt{x}$, where $C_{NM}$ is a constant depending on the semiconductor matrix and $x$ is the nitrogen composition.

It is evident from Eq. (1) that the initial rate of reduction in the N-induced band gap depends on the coupling parameter $V_{NM}$ and on the energy difference $E_M - E_N$. Therefore, the dependence of $E_N$, $E_M$, and $V_{NM}$ on the nitrogen content of the InPN bulk layer should be duly taken into account. Since GaAs and InP have similar energy gap and valence-band offsets (VBOs), it is natural to expect the BAC model to apply equally well to InPN.[23] We have derived a parameterization in which the GaAs/InP VBO was assumed to be 0.35 eV. Figure 3 shows an example of dispersion relations in InP$_{1-x}$N$_x$, calculated using Eq. (1) for $x = 0.002$. The parameters used in this calculation includes the reported values of $E_M(k=0) = 1.34$ eV of the InP matrix, the highly localized nitrogen level $E_N = 1.79$ eV (Ref. 23) relative to the top of the valence band maximum in InP, and the best fit value $C_{NM} = 3.5$ eV (Ref. 24).

Figure 4 plots the fundamental band gap, between the valence band maximum and the $E_-$ conduction band minimum, as a function of N fraction $x$ for InP$_{1-x}$N$_x$ at 300 K, calculated by the BAC model. As can be seen, our experimental data are somewhat in agreement, within errors, with the theoretical calculation from BAC model.
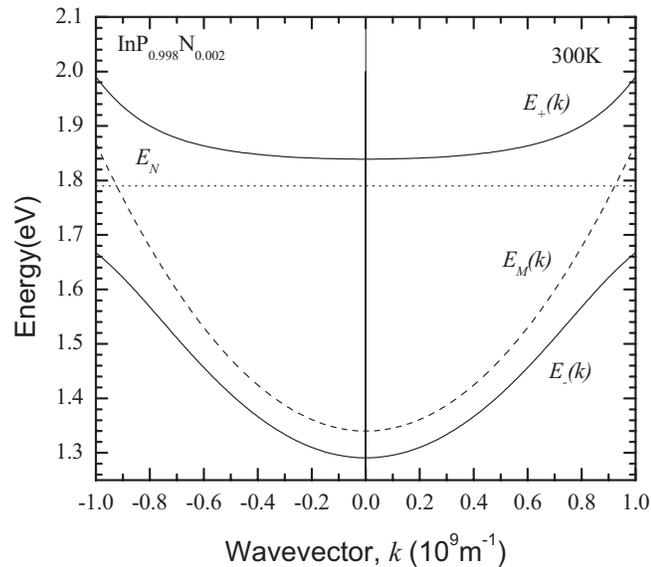
FIG. 3. Calculated dispersion curve for InPN.



FIG. 5. PL spectra for undoped LPE InP (solid line) and LPE $InP_{0.9994}N_{0.0006}$ (dotted line).

## C. Photoluminescence

PL spectra for a typical undoped InP layer, grown by LPE using the technique described earlier and a LPE InPN sample containing 0.06% nitrogen (as measured by optical absorption) are shown in Fig. 5. Spectrum for undoped InP is characterized by a broad peak with a maximum at 1.4253 eV, corresponding to free excitonic transitions in InP. For InPN, the free excitonic peak is narrower with the maximum at 1.4187 eV and a second peak at 1.3839 eV is clearly resolved. This indicates that the crystalline quality of the material is improved when nitrogen is introduced in the same. The peak at 1.38 eV has been observed earlier in InP and was attributed either to transitions from neutral donors to neutral acceptors $(D^0\text{-}A^0)$ (Ref. 25) or to the LO phonon replica of the free excitonic peak.[26] Comparing the major peaks of InPN and InP, we see that there is a marginal decrease of 6.6

meV in band gap due to nitrogen and this data more or less corresponds to that obtained for the same sample from absorption measurements at 300 K. The 1.38 eV peak is very weakly observed in a layer containing 0.2% nitrogen. However, when the sample is annealed for 40 min at 700 °C under hydrogen flow, the PL intensity is greatly increased enhancing the heights of both the 1.417 and the 1.383 eV peaks. These data are being shown in Fig. 6. The increase in luminescence after a postgrowth anneal was observed earlier in GaAsN (Refs. 27 and 28) and was attributed to the removal of point defects at high temperatures. This increase may also be partly due to the increase in substitutional nitrogen atoms and a corresponding decrease in interstitial nitrogen during annealing.[29] Such increase in substitutional nitrogen may also account for the observed slight redshift of PL peak after anneal.

## D. Electronic transport properties

Finally, in Fig. 7, we show carrier concentration and electron mobility for materials with varying amounts of
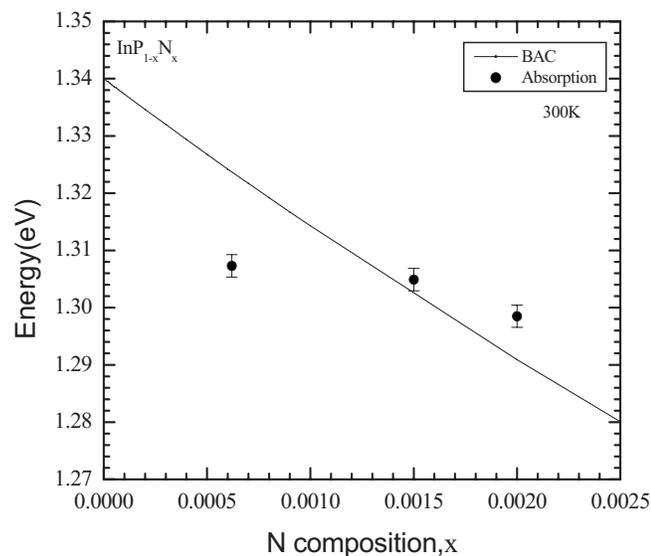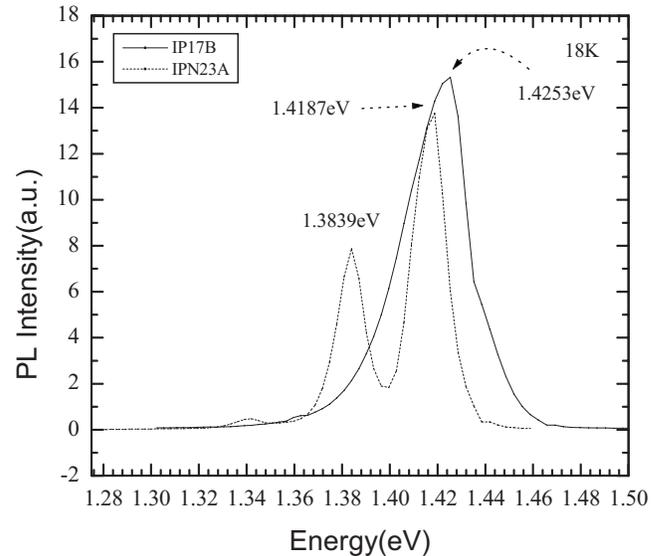


FIG. 4. Fundamental band gap of InPN calculated as a function of nitrogen composition using BAC model (solid line) and compared with our experimental data (solid circles).
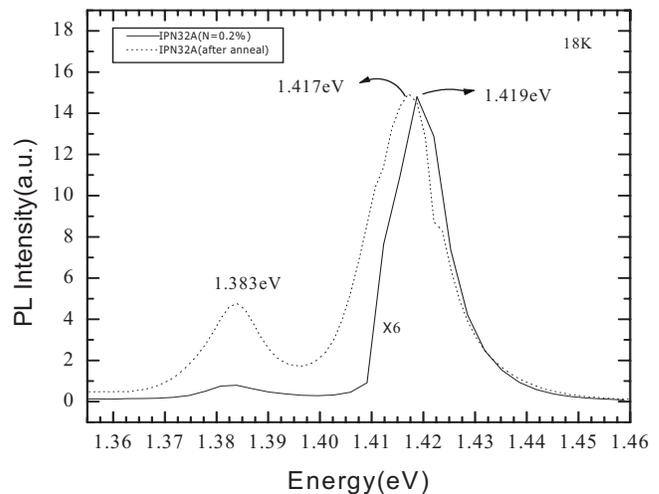


FIG. 6. PL spectra for LPE InPN (N: 0.2%) before and after an anneal at 700 °C for 40 min.
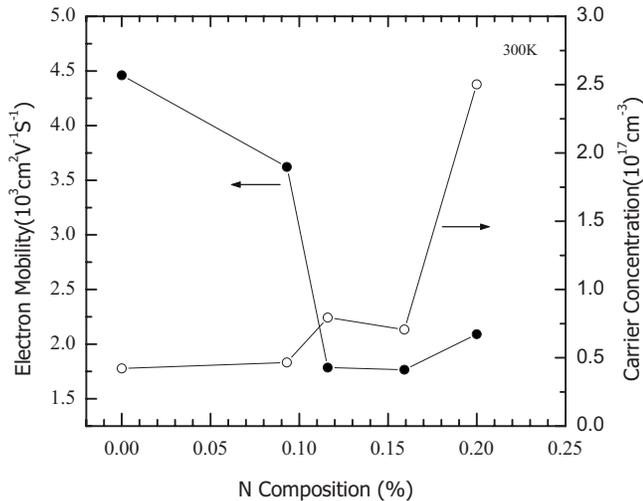
FIG. 7. Room temperature electron mobility and carrier concentration in LPE InPN as a function of nitrogen composition.

nitrogen. It is evident that there is a drop in mobility with a corresponding rise in carrier concentration as the nitrogen content in the material increases. The decrease in mobility may be due to an increase in ionized impurity scattering or due to scattering from nitrogen related scattering centers[30] or both.

## IV. CONCLUSION

Dilute InPN layers have been grown by LPE using polycrystalline InN powder as the source of nitrogen in the melt. By increasing the amount of InN in the growth melt, we were able to obtain a nitrogen content of up to 0.2%, as measured by high resolution XRD and room temperature optical absorption. PL from the nitrogen containing material showed narrower peaks as compared to that from undoped LPE InP and indicated the existence of a 1.38 eV emission. Mobility of the layers consistently decreased with increase in nitrogen content. The luminescence also greatly improved under a postgrowth anneal of the layers.

## ACKNOWLEDGMENTS

[1] W. G. Bi and C. W. Tu, Appl. Phys. Lett. **70**, 1608 (1997).
[2] E. V. K. Rao, A. Ougazzaden, Y. Le Bellego, and M. Juhel, Appl. Phys. Lett. **72**, 1409 (1998).
[3] H.Ch. Alt, A.Yu. Egorov, H. Riechert, B. Wiedemann, J.D. Meyer, R.W. Michelmann, and K. Bethge, Appl. Phys. Lett. **77**, 3331 (2000).
[4] A. Ignatov, A. Patane, O. Makarovsky, and L. Eaves, Appl. Phys. Lett. **88**, 032107 (2006).
[5] M. Kondow, K. Uomi, A. Niwa, T. Ktatani, S. Watahiki, and Y. Yazawa, Jpn. J. Appl. Phys., Part 1 **35**, 1273 (1996).
[6] G. Ungaro, G. Le Roux, R. Teissier, and J. C. Harmand, Electron. Lett. **35**, 1246 (1999).
[7] W. Li, J. B. Heroux, and W. I. Wang, J. Appl. Phys. **94**, 4248 (2003).
[8] K. Yamamoto, M. Uchida, A. Yamamoto, A. Masuda, and A. Hashimoto, Phys. Status Solidi B **234**, 915 (2002).
[9] A. Polimeni, M. Bissiri, M. Felici, M. Capizzi, I. A. Buyanova, W. M. Chen, H. P. Xin, and C. W. Tu, Phys. Rev. B **67**, 201303(R) (2003).
[10] S. A. Lourenco, I. F. L. Dias, L. C. Pocas, J. L. Duarte, J. B. B. de Oliveira, and J. C. Harmand, J. Appl. Phys. **93**, 4475 (2003).
[11] D. K. Shih, H. H. Lin, L. W. Sung, T. Y. Chu, and T. R. Yang, Jpn. J. Appl. Phys., Part 1 **42**, 375 (2003).
[12] C. W. Tu, J. Phys.: Condens. Matter **13**, 7169 (2001).
[13] W. Shan, W. Walukiewicz, K. M. Yu, J. Wu, J. W. Ager III, E. E. Haller, H. P. Xin, and C. W. Tu, Appl. Phys. Lett. **76**, 3251 (2000).
[14] W. G. Bi and C. W. Tu, J. Appl. Phys. **80**, 1934 (1996).
[15] K. M. Yu, W. Walukeiwicz, J. Wu, J. W. Beeman, J. W. Ager III, E. E. Haller, W. Shan, H. P. Xin, and C. W. Tu, Appl. Phys. Lett. **78**, 1077 (2001).
[16] M. Debbichi, A. Ben Fredj, A. Bhouri, N. Bouarissa, and M. Said, Eur. Phys. J. B **51**, 17 (2006).
[17] S. Dhar, N. Halder, J. Kumar, and B. M. Arora, Appl. Phys. Lett. **85**, 964 (2004).
[18] S. Dhar, N. Halder, and A. Mondal, Semicond. Sci. Technol. **20**, 1168 (2005).
[19] A. Mondal, T. D. Das, N. Halder, S. Dhar, and J. Kumar, J. Cryst. Growth **297**, 4 (2006).
[20] S. Dhar, T. D. Das, M. de la Mare, and A. Krier, Appl. Phys. Lett. **93**, 071905 (2008).
[21] J. Wu, W. Shan, and W. Walukiewicz, Semicond. Sci. Technol. **17**, 860 (2002).
[22] W. Shan, W. Walukiewicz, J. W. Ager III, E. E. Haller, J. F. Geisz, D. J. Friedman, J. M. Olson, and S. R. Kurtz, Phys. Rev. Lett. **82**, 1221 (1999).
[23] K. M. Yu, W. Walukiewicz, J. Wu, T. W. Beeman, J. W. Ager III, E. E. Haller, W. Shan, H. P. Xin, and C. W. Tu, Appl. Phys. Lett. **78**, 1077 (2001).
[24] I. Vurgaftman and J. R. Meyer, J. Appl. Phys. **94**, 3675 (2003).
[25] L. D. Zhu, K. T. Chan, D. K. Wagner, and J. M. Ballantyne, J. Appl. Phys. **57**, 5486 (1985).
[26] A. M. White, P. J. Dean, l. L. Taylor, R. C. Clarke, D. J. Ashen, and J. B. Mullin, J. Phys. C **5**, 1727 (1972).
[27] S. Francoeur, G. Sivaraman, Y. Qiu, S. Nikishin, and H. Temkin, Appl. Phys. Lett. **72**, 1857 (1998).
[28] J. S. Wang, A. R. Kovsh, L. Wei, J. Y. Chi, Y. T. Wu, P. Y. Wang, and V. M. Ustinov, Nanotechnology **12**, 430 (2001).
[29] T. Ahlgren, E. Vainonen-Ahlgren, J. Likonen, W. Li, and M. Pessa, Appl. Phys. Lett. **80**, 2314 (2002).
[30] S. Dhar, A. Mondal, and T. D. Das, Semicond. Sci. Technol. **23**, 015007 (2008).